Research Article – Vol. 01, Issue 03, No. 03

Advanced in Engineering and Intelligence Systems

Journal Web Page: https://aeis.bilijipub.com

Utilizing the Novel developed MLP Techniques to Survey Pile Subsidence via Optimization Algorithms

Augustinus Sieck[1,*] , Graciela Daniels[2]

[1] *The King's School, Bujumbura BP1560, Burundi*
[2] *Central Arizona College, Coolidge 85128, AZ, United States*

Highlights

- Subsidence rate visualization using artificial neural network methods.
- Using Multilayer Perceptron coupled with the optimizers for the Pile Subsidence study.
- Improvement of Multilayer Perceptron performance by employing Arithmetic Optimization Algorithm and Biogeography-Based Optimization.
- To test the piles, 'The Klang Valley Mass Rapid Transit network built in Kuala Lumpur.
- The R^2 value of MLP-AOA and MLP-BBO were obtained at 0.93 and 0.94, respectively.

Article Info

Received: 26 July 2022
Received in revised: 15 September 2022
Accepted: 15 September 2022
Available online: 01 October 2022

Keywords

Arithmetic Optimization Algorithm;
Pile Settlement Estimation;
Biogeography-Based Optimization;
Multilayer Perceptron;
Artificial neural network;
Malaysia

Abstract

The Pile settlement (PS) is one of the most essential issues in designing piles and its foundation type applied in real state. Over the variants in designing the pile penetrated in rock, the vertical settlement is of paramount importance to know. However, rigorous theoretical descriptions for soil-pile interactions are still ambiguous. In this regard, most research has tried to figure out the subsidence rate in piles after loading overtime via artificial intelligence methods. The Artificial Neural Network, as a widespread method, has absorbed attention to draw the actual picture of pile movement vertically during the loading period. This research aims to develop the Multilayer Perceptron coupled with the Novel Arithmetic Optimization Algorithm and Biogeography-Based Optimization to find out the optimal number of hidden layers of neurons within MLP. The Klang Valley Mass Rapid Transit network built in Kuala Lumpur, Malaysia, was chosen to test the piles' settlement and earth properties algorithms. In the prediction process, the R^2 value of MLP-AOA and MLP-BBO were obtained at 0.93 and 0.94, respectively. The measured range of piles movement was from 4.5 to 20 centimeters, which predicted settlements showed us an average one percent change compared to measured magnitudes.

1. Introduction

The extreme requirement to design a pile and its foundation has been an outstanding matter with the fast growing tall and heavy constructions and structures worldwide. Subsequently, accurate estimations of pile settlements have turned to be more important. Pile settlement (PS) rates, Moreover, under diverse load compositions are obviously available from the in-situ experiments that are completely applicable but most of the time costly and difficult to perform. Generally, Pile Settlement (PS) is defined through the pile length, pile load, shear modulus, the width of pile cross-section, as well as radial distance in which the shear stress seems ignorable [1]. Specifically, the variant of UCS used for rocks is strictly corresponding to the pile capacity, which influences PS as well as the leading factor affecting the magnitude of PS, namely N_{SPT} [2] _[3].

For this reason, many simplified theoretical methods have been developed to estimate pile movement overloading. In the relevant literature, Coyle and Reese [4] introduced the load transfer method, in which the relationship between the pile element displacement and the friction of soil is established. Zhang and Zhang [5] further

* Corresponding Author: Augustinus Sieck
Email: augustinussieck@ksu.edu.bi

developed this model to conduct nonlinear analyses. Although the load transfer method is mathematically easy to run, it simplifies the soil behavior as discrete springs for which a large number of parameters need to be acquired from field experiments [6]. In particular, the model could not perform well once the soil condition is complex [7]. Besides, the coefficients of soil strength are related to pile displacement instead of soil fundamental movement, which multiplies the difficulty of getting relative coefficients [8]. Also, to appraise a rigorous method of pile settlement, Poulos and Davis (1980) considered the pile as an incompressible tough component and acquired a numerical solution of pile end settlement using the integral transformation method [9].

Besides these methods as intelligent ways, Shahin [10] utilized neural networks calibrated with in-situ full scale pile load experiments estimating pile settlement rates. Other studies were mostly targeted at solving problems such as the gain in bearing capacity or the loss due to pile driving, post-pile displacement due to negative skin friction, and pore pressure development [11]–[15]. Other present regression ways were utilized widely and correctly,such as Gaussian process regression, multivariate adaptive regression spline (MARS), minimax probability machine regression[16]–[22]. Also, the Genetic Expression Programming (GEP) way to a way tied to the axial capacity of piles was taken into account [23]. Additional research studied three algorithms of multilayer perceptron, machine of support vector, and GEP to estimate the UCS parameter for rock [24].

Goh [25] applied neural network base solutions to formulate the outputs of settlement behavior of piles. The training data set was gathered from real pile derived registrations. The developed networks could estimate the results more reliable and consistent. Teh et al. [26] used neural network models to estimate pile-bearing capacity. The significant data set utilized to train the network of database compiled of 37 concrete piles was collected from 21 different construction sites.

Some models for data mining were developed to forecast the subsidance of the foundation concurring to standard test values for penetration. Approximately, researchers used a thousand gained from researches on the way to magnify the model containing ground estimations [27]. Using the Artificial Neural Network (ANN) to guess the movement of raft foundations for noncohesive-soil was produced, entering variables were composed of soil features, footing dimensions, align with the strengthening specifications from each test or ground estimation [28].

Accordingly, the parameter of UCS for rock sorts, the ratio of length for pile to pile-diameter, loads over pile, the ratio of length in the pile in soil to rock, and N_{SPT} are neccasary entring variables to estimate the settlement of rock socketed piles into earth [29]. The application of technique data mining has been explained in researches to solve geotechnical matters by model expanding [30] _ [35]. To this end, the present research has eagerly studied the use of developed Multilayer Perceptron (MLP). In fact, in addition to this technique, applying the proposed optimizer to figure out the optimal number of hidden layers of neurons would be the novelty of this research. Optimization algorithms enhance the accuracy of these tools by overcoming the mentioned problems [36]. Arithmetic Optimization Algorithm (AOA) and Biogeography-Based Optimization (BBO) would be this research proposed optimizers to couple with MLP. Moayedi et al. [36] used a BBO optimizer to integrate with MLP to assess landslide susceptibility. In the outcome, the application of BBO metaheuristic algorithms enhanced the accuracy of the MLP to find the most appropriate computational variables of ANN assigned to the conditioning factors. The AOA state-of-art optimization algorithm has been introduced recently, operating by some academic fields, indicating high performance and improving the modeling process [37]– [39].

The yields come about the desirability of the MIP-BBO method in corresponding research, through MAE on 0.1378 validation stage, which shows us the usefulness of this edition to estimate PS [40]. Various research aimed to develop an MLP framework picked up from a computation correlated with the BBO and novel AOA algorithms to foresee PS.

Regarding the goal of this research, it is worth noting that this article utilizes the optimization algorithms, AOA and BBO coupled with a neural network named MLP-AOA and MLP-BBO to determine the optimal determinative numbers of neurons of hidden layers in multilayer perceptron.

For the research case, parameters, as the pile length embedded in soil to length beneath the rock subsurface ratio, the capacity of final bearing as the factor of input, along with PS as yield. For evaluating the correctness of the models planned, uniaxial compressive strength, whole length to diameter, standard penetration test, the indices of RMSE, MAE, VAF, and R^2 were used.

The novelty of this research is the specified algorithms foreseeing the PS in rock. To use the abovementioned algorithms, the tests reports for pile driving analysis and the properties of ground had been measured for the Transport network project of Klang Valley Mass Rapid (KVMRT) transportation network operating in the country of Kuala Lumpur, the city of Malaysia.

2. Methodology

2.1.Initializing Dataset

The transport network project of Klang Valley (KVMRT) in the country of Kuala Lumpur, the city of Malaysia, to decline traffic congestion was chosen as a case study. Such projects have exhibited that a large quantity of socketed pillars are essential supporting the bases to avoid failure and to analyze the performance of piles collecting primitive data. The project location as study area is domenstrated through Fig. 1 in which a great number of piles are established on various rock stations such as limestone kind or phyllite, and granite.

The characteristics of 96 piles constructed by granite rock-based have considered in this research. The the San Trias type of granite rock was seemed in the area. Data and beneath the ground materials at the pile site covered the dominating geological properties. The beneath soil layers are collected from remaining pieces of rocks as in the results. Accordingly, in the data gathered, the bed rock depth is estimated to be in a span of 70 cm to more than the threshold of 1400 m below. Besides, the process of sampling and information of socketed pillar have brought in the lines as follow:

a) The mass of observed rocks among moderately to extremely weathered ones
b) Undermost and top rates of UCS according to the ISRM parameter, respectively, at the level of 25 and 68 Mega Paskal, [41].
c) Log data of bore in the 16.5 meters, extremely weathered soil, and the dominant sort of soil is made up of mostly mud including sand plus a atleast and atmost 4 and 167 of N_{SPT} lower per 300 mm, respectively.
d) A large region under the surface depth in the range between 7.5 and 27.0 meters, underground context with N_{SPT} rate further than 50 deep per 300mm.

Preparing initial information with entering inputs seems the primitive phase for estimating the outputs. Determining the factors impacting the model output is compulsory to the proposed framework. The empirical expriments abovementioned were done by Dynamic of Pile, Inc, applying a pile analysis. It was also previously noted that length of pile and crosssection pile diameter are the variables for the forcasting of pile movement quantity in the pile movement. Therefore, both variant, called the length of pile below the soil to length of pile under the rock proportion (L_s/L_r), and the total length of pile-to-pile diameter (L_p/D) got opted to investigate the status of geometryof pile on settlement. The magnitude of N_{SPT} was similarly was enrolled entring input to demonstrate the status of the soil. Further, the parameter of UCS was considered as input of the model for pillar movement estimation. In addition, the load over pile has a straight effect on the pile movement. Therefore, the last bearing capacity of pile (Q_u) got recognized entering data. variables got opted for appraising pile settlement (PS). The entering data and outcomes from the model in this study, align with revealed ranges, have being indicated by Table 1. The graphs of entering data and target (PS) have been brought through Fig. 1 as well.

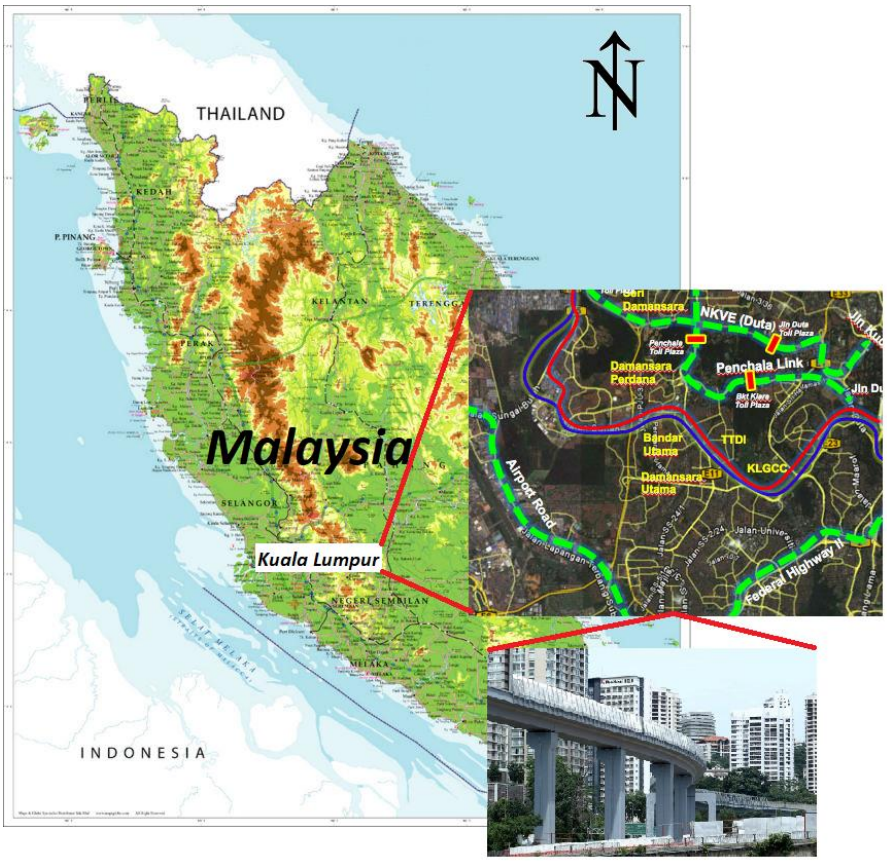

Fig. 1. The project of KVMRT transportation network

Table 1. The statistical values of the input and output variables.

Class	Parameter	Symbol	Min.	Max.	Median	St. Dev	Avg.
Input	Soil length to socket length ratio	L_s/L_r	0.3	32	4	7	7
	The ratio of total length to diameter	L_p/D	4	32	14	7	15
	Uniaxial compressive strength	UCS (MPa)	25	68	43	12	43
	Standard penetration test	N_{SPT}	3	166	104	59	80
	Ultimate bearing capacity	Q_u (KN)	12409	42701	21898	8030	24540
Target	Pile settlement	PS (mm)	4.50	20.10	11.00	3.70	11.00

As shown from Fig. 2, these scatter plots have tried to show the relationship of each effective independent parameter and indicate each range in which Lp/D, Ls/Lr, and Qu are recognized to increase pile settlement, enhancing them. However, the variables of N_SPT and UCS have an inverse relationship with PS.

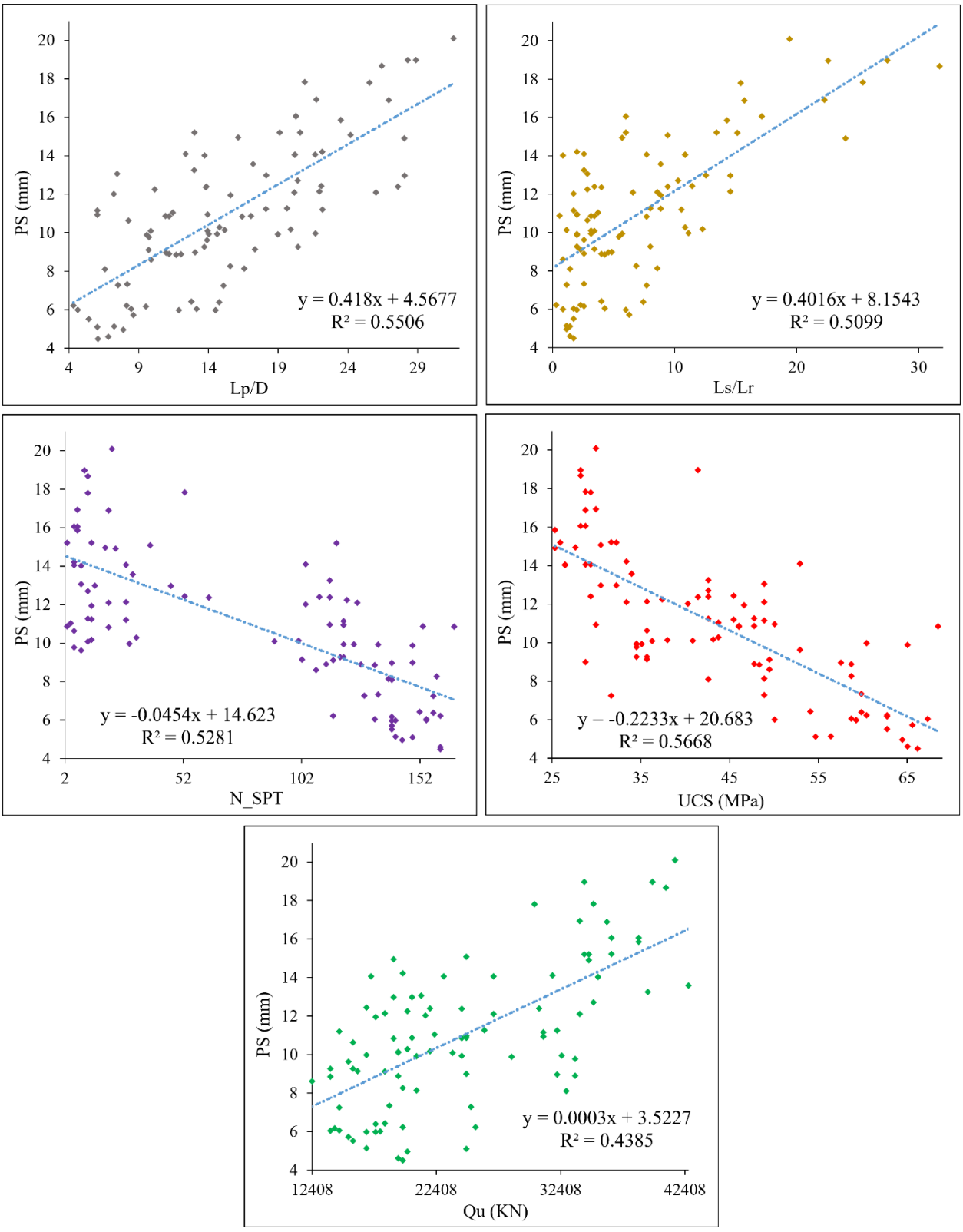

Fig. 2. The dataset for the training and testing phase

2.2. Arithmetic optimization algorithm (AOA)

AOA is a candidate-based algorithm with an algebraic pattern that involves arithmetic operators to check and

boost the new state of the population without considering their derivatives [42]. Arithmetic is the main part of present mathematics and seems one of the number theories bases algorithm procedures that commences with initializing the candidate solutions, which are made randomly. Eq.(1) shows the initial candidates matrix.

$$C = \begin{bmatrix} c_{1,1} & \cdots & c_{1,j} \\ \vdots & \ddots & \vdots \\ c_{N,1} & \cdots & c_{N,j} \end{bmatrix} \quad (1)$$

The algorithm comprises two main parts of exploration and exploitation [42]. After creating the initial candidate, the exploration or exploitation finding area should be defined and conducted by the math optimizer accelerator function (MOA) Eq (2).

$$MOA = Min + iter \times (\frac{Max - Min}{Max_{iter}}) \quad (2)$$

Where Min and Max represent the minimum and maximum MOA values. The $iter$ is the current iteration and Max_{iter} denotes the maximum iteration number.

The exploration search stage is performed by high distributed values using multiplication (M) and division (D) arithmetic operators to the exploration search action. Operators M and D create a high dispersion that cannot help reach the target. However, applying subtraction (S) and addition (A) operators in the exploitation stage results in getting the best target [42].

If the $r_1 > MOA$ is true, the exploration stage of the algorithm is in process. The state in the exploration stage is upgraded using Eq. (3), the benefits from M and D operators.

$$c(iter+1)_{i,j} = \begin{cases} best(c_j) \div (MOP + \varepsilon) \times ((ub - lb) \times \mu + lb) & r_2 > 0.5 \\ best(c_j) \div (MOP) \times ((ub - lb) \times \mu + lb) & otherwise \end{cases} \quad (3)$$

Where appropriate (c_j) is the global best position, ub, and lb shows the upper and lower bound of the search area. The parameter of ε shows a little value, and μ is the adjusting control parameter of the search procedure set to 0.499 in this research. The MOP is determined as a math optimization probability calculated as Eq. (4).

$$MOP(iter) = 1 - \frac{iter^{1/\alpha}}{Max_{iter}{}^{1/\alpha}} \quad (4)$$

In this equation, the variable of α represents the sensitivity parameter of exploitation accuracy throughout the iterations Eq. (5).

Also if $r_1 < MOA$ the exploitation stage happens in this stage, S and A arithmetic operators are applied for a deep search of the dense area. This deep searching is modeled as follows [42].

$$c(iter+1)_{i,j} = \begin{cases} best(c_j) - (MOP) \times ((ub - lb) \times \mu + lb) & r_3 > 0.5 \\ best(c_j) + (MOP) \times ((ub - lb) \times \mu + lb) & otherwise \end{cases} \quad (5)$$

2.3. Biogeography-based optimization (BBO)

The BBO metaheuristic algorithm is inspired by geographical distribution and immigration within the ecosystem [43]. In the optimization algorithm, the assumed ecosystem should contain a limited number of habitats. Different parameters called suitability index variables influence each habitat quality for species, including food, water resources, climate condition, etc. Another criterion is the habitat suitability index (HSI) to represent the quality of each habitat. If a habitat is filled or has an enormous HSI, the species tend to immigrate from the habitat and immigrate to the small HSI value. Each living location supplied a feasible solution, and its suitability index is the decision variable (DVs). Over the optimization process, the solutions with lower values for objective have a larger magnitude of HSIs. Two operators called "migration" and "mutation" are being used in the mentioned algorithm. The migration operator is applied to find the proximity of the existing responses, and the mutation one is used to explore the new answers and help with the exploration.

For the sake of habitat with the size of habitat suitability, the habitats are listed from their cost function values. The suitability of the i^{th} habitat (HSI_i) in the sorted generation is specified as Eq. (6).

$$HSI_i = -i + HS + 1 \quad (6)$$

The emigration (μ_i) and immigration (λ_i) values are given through Eq. (7) and Eq. (8).

$$\mu_i = \frac{HSI_i}{HS} \quad (7)$$

$$\lambda_i = 1 - \frac{HSI_i}{HS} \quad (8)$$

Fig. 3 shows the migration process of the BBO. Here, the largest value of emigration and immigration speed is assumed to be one. Migration from the j^{th} decision variable of r^{th} habitat to the decision variable of i^{th} habitat computed through Eq. (9).

$$DV_j^k = \alpha DV_j^i + (1-\alpha)DV_j^r \quad (9)$$

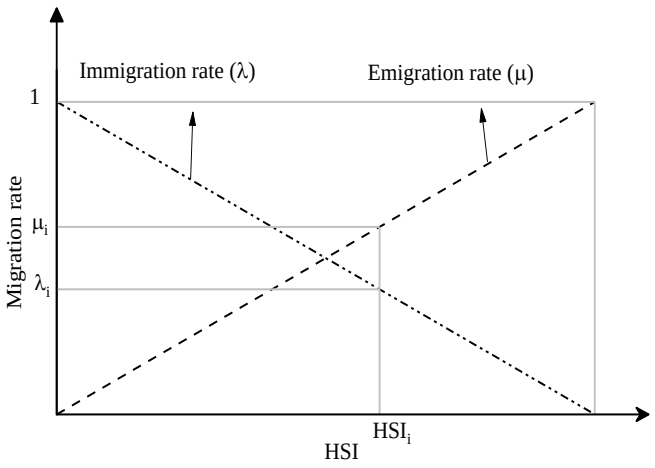

Fig. 3. Migration curve of the BBO.

2.4. Integrated neural network models, MLP-BBO and MLP-AOA

A Sigmoid base function neural network is used as a feed-forward network, including the input, hidden, and output layers. In this regard, the convergence speed rate is appropriate [44]. The input nodes enter variables to the hidden layer, which a sigmoid activation function shapes the hidden layer nodes. This neural network responds to the input signals according to defined classes. The resulted output of the hidden layer is transmitted to the output layer, which mainly employs a simple linear function [45].

Fig. 4 represents the structure of MLP-BBO and MLP-AOA models. These coupled models are adjustable techniques that automatically dedicates the hidden layer neuron number. Each layer includes neurons by special mathematical algorithm relationships, but the number of output layer neurons depends on the objective dataset. The neurons of the hidden layer have been recognized in charge of realizing and finding the speces based on the internal signals transferred. The stage next has been done for the hidden layer: Getting the entering layer neurons and assigning their summation weighted, plus the addition of biases to summation weighted, spotting the outcomes from the phase of second into function of transfer, then sending outcomes to the last end layer of output or the hidden layer of next.

For this research, the highest number of hidden layers was assigned 30, although the number of hidden layers as an arbitrary variable tried to the maximum three layers. By same token, the algorithms of AOA and BBO are operated to model by diverse hidden layers (one - three layers) to ascertain the optimized number of neurons for each hidden layer. Many algorithms have been explored in the ANN training method for obtaining weight and bias. To this end, the back-propagation algorithm for MLP learning is utilized based on previous successful researches [46], [47]. For the method, the entering data feeded with signals are shifted and weighted amongst diverse number ofneurons in layers to be given the plausible output. The developed MLP mechanism is depicted through Fig. 4.

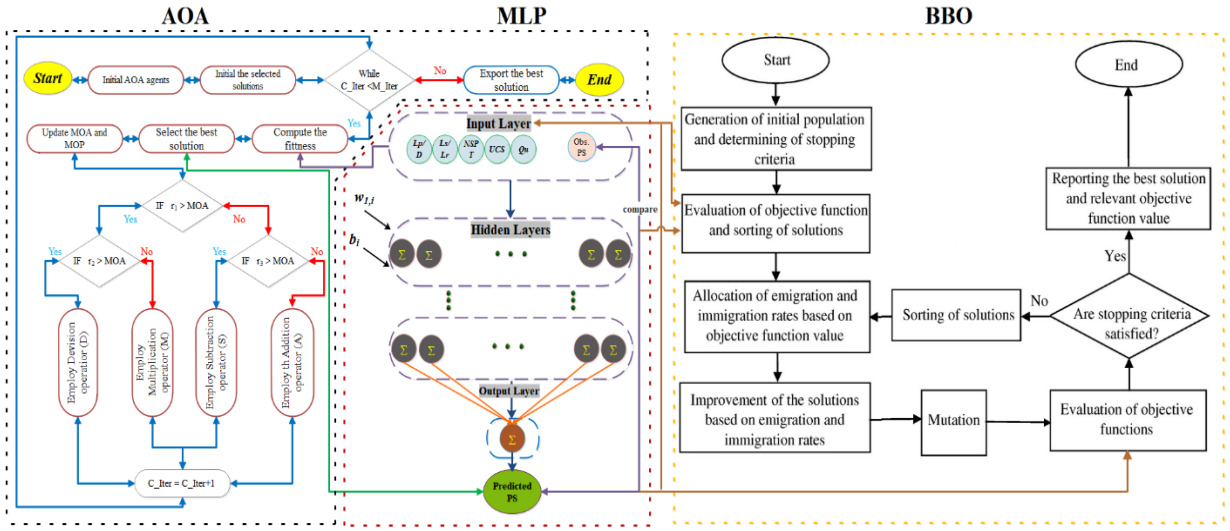

Fig. 4. Flowchart of developed MLP-BBO, MLP-AOA

2.5. Evaluation of model performance

The performance criteria for evaluating the developed platform are introduced in Table 2:

Table 2. The performance evaluation indices

Index name	Symbol	Equation	Description
Coefficient of determination	R^2	$\left(\frac{\sum_{n=1}^{N}(t_n-\bar{t})(p_n-\bar{p})}{\sqrt{[\sum_{n=1}^{N}(t_n-\bar{p})^2][\sum_{n=1}^{N}(p_n-\bar{p})^2]}}\right)^2$	Higher is better
Root mean squared error	RMSE	$\sqrt{\frac{1}{N}\sum_{n=1}^{N}(p_n-t_n)^2}$	Lower is better
Mean absolute error	MAE	$\frac{1}{N}\sum_{n=1}^{N}\lvert p_n-t_n\rvert$	Lower is better
Variance account factor	VAF	$\left(1-\frac{var(t_n-y_n)}{var(t_n)}\right)*100$	Higher is better

where, $p_N, t_N, \bar{t}, \bar{p}$ indicate the estimated magnitude of N^{th} paradigm, the objectiver amounts relavent to the N^{th}, the target values averages and, respectively, that of the estimated magnitudes.

3. Result and discussion

The outcomes of the developed integrated MLP models (i.e., MLP-BBO and MLP-AOA) to forecast the pile settlement are indicated in this section. Fig. 5 presents the scatter plot between observed and predicted PSs for both developed models, the correlation of determination figures, and their error in the testing stage. All three layers in separate modeling showed the depicted results in Fig. 5. As can be seen from the figure, the performance of the BBO in optimizing neuron process seems more accurate than AOA, especially in three hidden layers type modeling due to R^2 being equals to 97 percent. On the other side, the MLP-AOA showed weaker activity by increasing *RMSE* in each modeling that the best one happened in one hidden layer modeling with 1.05. However, the whole modeling showed a great correlation of higher than 90 percent R^2. Also, through eyes, it is clear that green square points representing the MLP-BBO are well laid out on and close to the bisector. Moreover, the modeling of pile settlement in the three layers status shows a best-fit line depicting low subsidence rates.

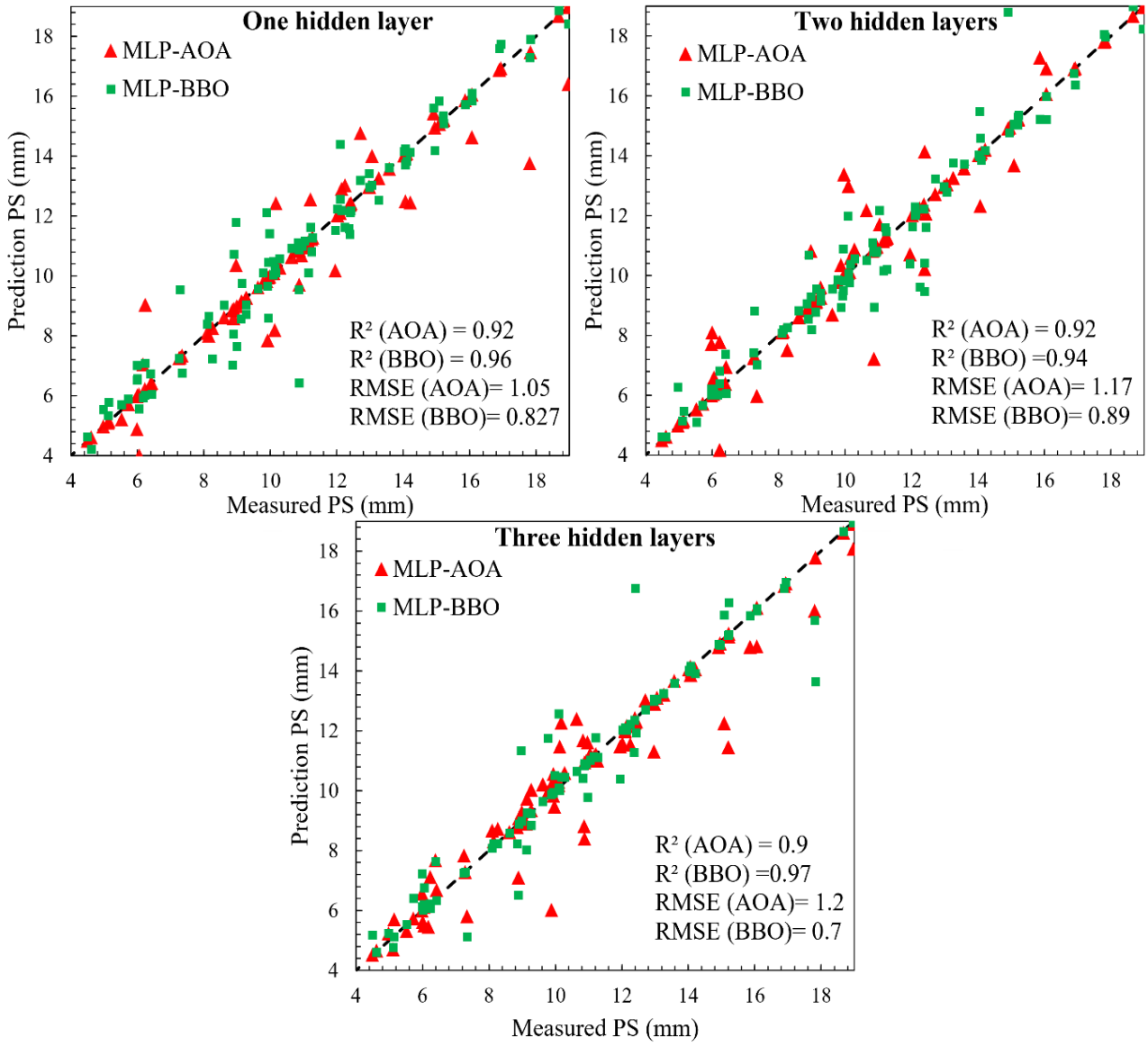

Fig. 5. Correlation and error of modeling both MLP-BBO and MLP-AOA

To elaborate the modeling process by evaluating the testing and training phase modeling through indices in Table. The overview of modeling efficiency can be completed using different evaluators. Fig. 6 and 7 separately show the training and testing model, respectively, for the various hidden layers used in models. The R^2 of the training phase for the MLP-AOA in one layer shows the best correlation (0.955) rather than other hidden layer number status and MLP-BBO (a). While the MLP-BBO shows the lower number for R^2 in the three hidden layers state (R^2 =0.923). *RMSE* (b) indicator shows a weak performance of the BBO optimizer compared to the AOA. That the best value of *RMSE* belongs to MLP-AOA framework in the condition with one hidden layer as reaches to 0.779 and the large value is assigned to MLP-BBO with the *RMSE* equals to 1.007 in three hidden layer modeling. By the same token, for the *MAE* (c), the BBO optimizer has been given low performance in modeling each status of one, two, and three hidden layers. In the training phase, there is another evaluator as proof that helps us know the productivity of each optimization algorithms. The *VAF* (d) index shows the better activity of the AOA performance except for the two layers condition that BBO seems to be better with 94.44.

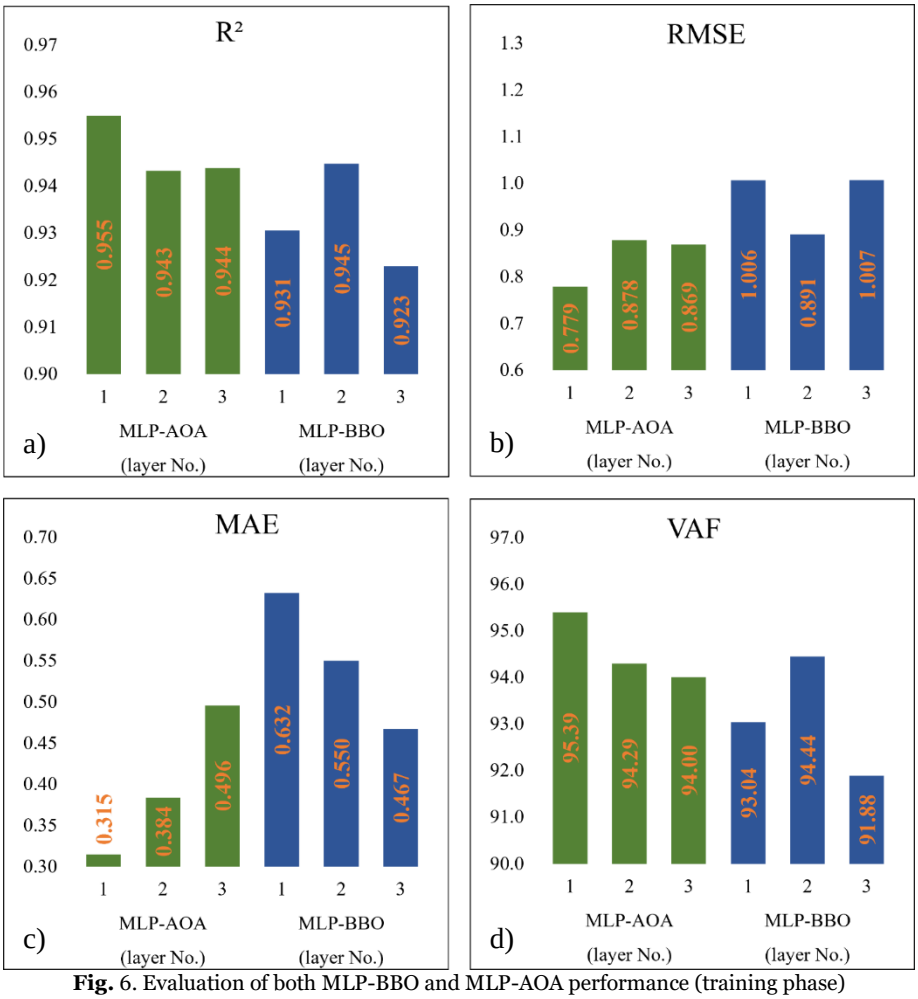

Fig. 6. Evaluation of both MLP-BBO and MLP-AOA performance (training phase)

Fig. 7 indicates the different story of modeling results for the testing phase, opposite to the results of Fig. 6, in which the MLP-BBO has an outstanding performance, and it would be at a top-level of modeling with the excellent rates that have been given through different criteria. The R^2 of MLP-BBO in each modeling type in terms of the number of hidden layers is placed in a better range than in three hidden layer conditions. The correlation of 97 percent is a higher magnitude we can see among others (a). The error of modeling by AOA optimizer mentions the weaker performance of this optimizer for each modeling type that in three hidden layers condition the *RMSE* show the 0.699 for the BBO while the large error number of 1.055 for AOA optimization algorithm (b). This trend, also, can be found in the *MAE* index (c) that in the best condition, the MLP-BBO framework denotes the 0.325, while in the testing stage, the MLP-AOA framework gets 0.695 which is two-fold the BBO, in the three hidden layers modeling. The indicator of *VAF*, in addition, shows the efficient performance of the BBO by reaching the value of 96.66 compared to 90.33 for the AOA in the three hidden layers modeling (d).

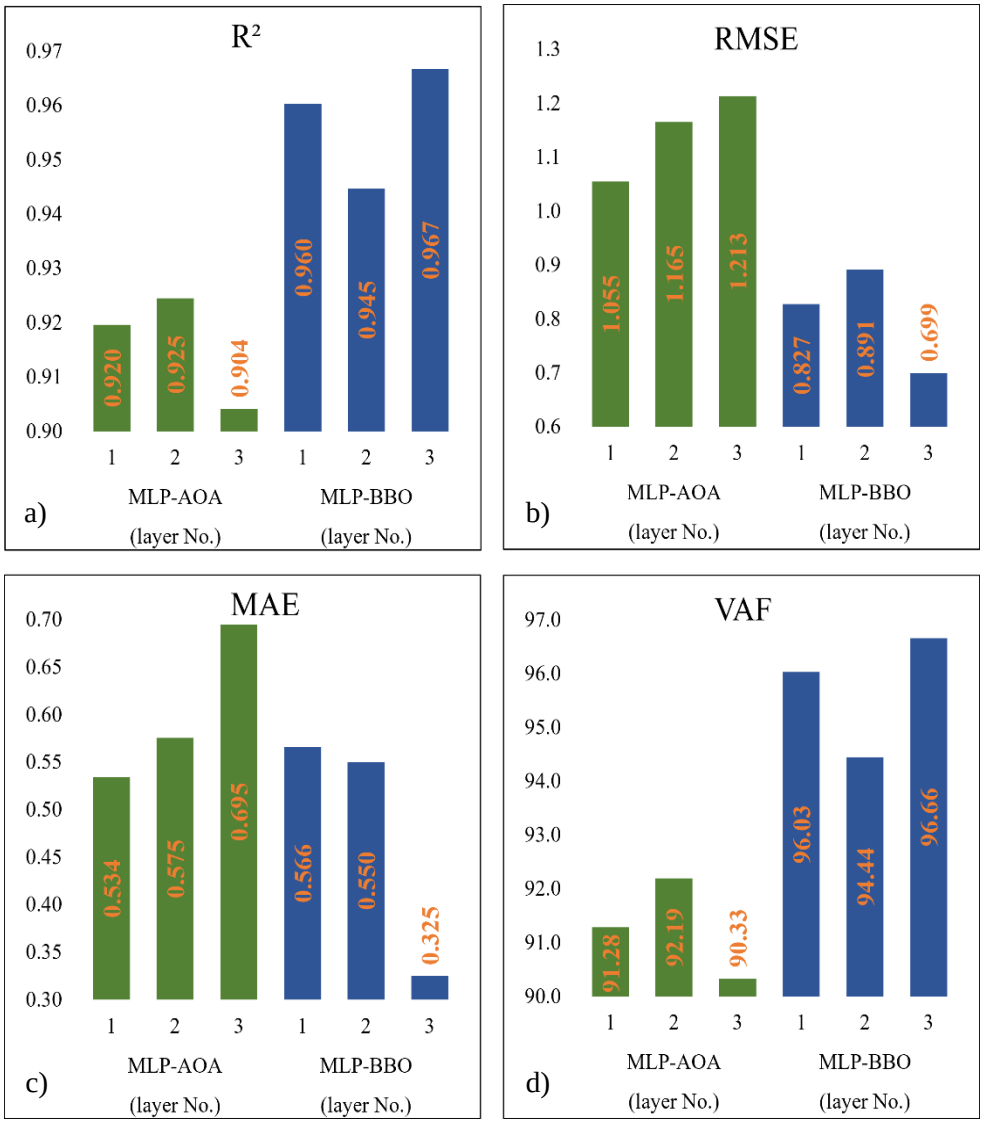

Fig. 7. Evaluation of both MLP-BBO and MLP-AOA performance (testing phase)

The other analysis must monitor the error percent per pile that the actual movement rate deviates from the model. Respectively, Fig. 8 has tried to exhibit the power of each type of modeling in terms of hidden layer numbers (a, b, and c) to compare either of the models in modeling the pile settlement.

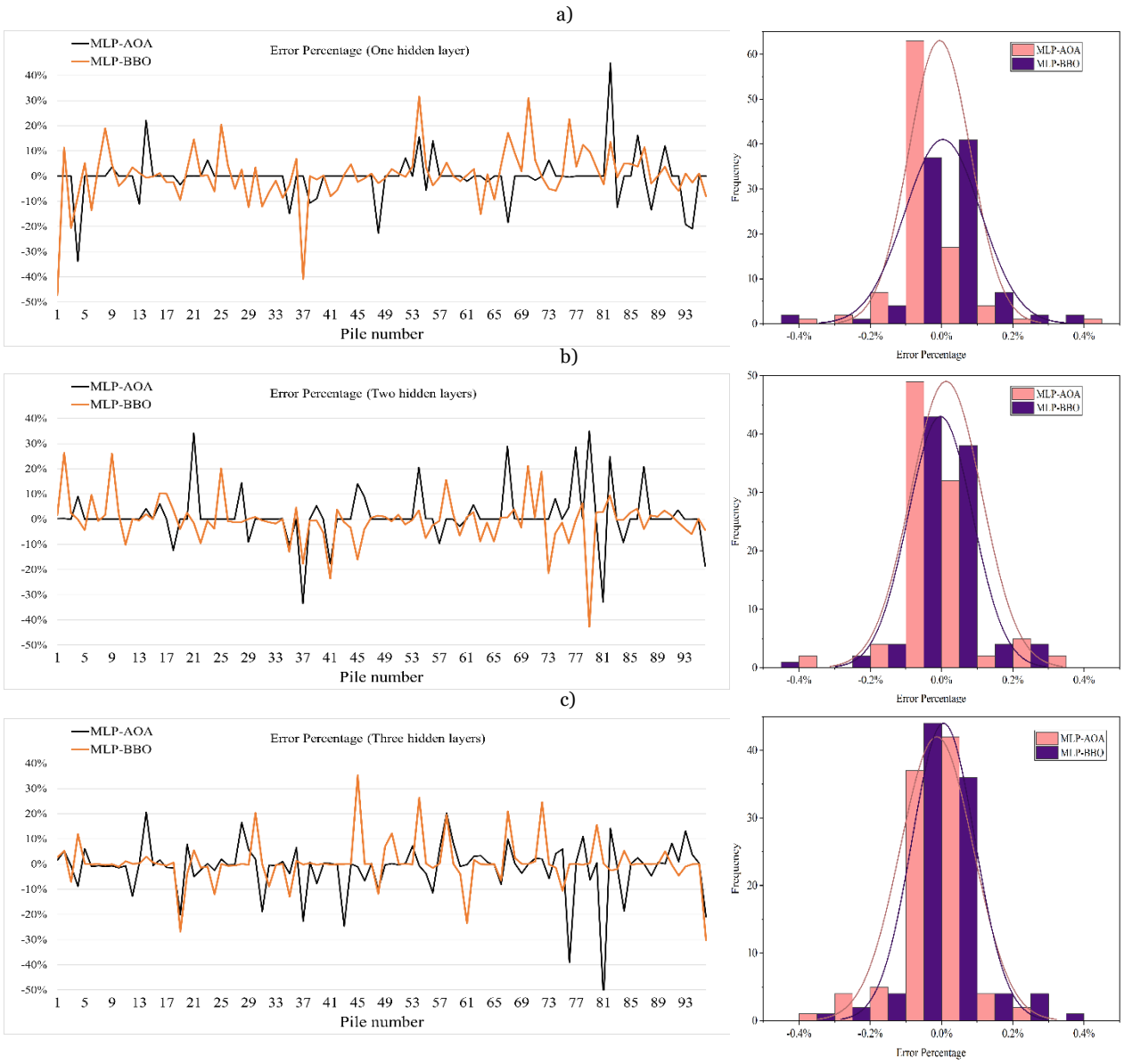

Fig. 8. The error of modeling MLP-BBO and MLP-AOA frameworks

The graphs in Fig. 8 show the deviations of errors according to each pile (left diagrams), and the right ones indicate the normal distribution of modeling error compared to each other.

Graphs of group "a" that denote the pile settlement modeling with one hidden layer show the same modeling trend for both MLP-BBO and MLP-AOA in terms of error signs. But based on a standard distribution of errors, the large gap between the two models is bold to the eye that the BBO optimizer has gained better operation for modeling PS. For graph group "b," the pile subsidence estimation with the low number of piles has the same modeling results, but for the last ones, there are completely different modeling results that both models have two opposite outcomes in some cases. The same diagrams are also seen with bell shapes in the normal distribution of two hidden layers modeling. For the graphs class "c," the modeling results are identical to each other, and the normal distribution of errors has a little gap. Moreover, the errors related to modeling the piles with the low numbers have been in accordance in even some cases. However, there are inverse results in the last number of piles as underestimation and overestimation.

Finally, the optimal number of neurons in ANN for each hidden layer is calculated through proposed optimization algorithms. Regarding the complexity of

neural networks and the cost of computations by increasing the hidden layers, each optimizer has aimed to minimize the abovementioned factors that Table 3 has indicated for both AOA and BBO optimization algorithms.

Table 3. The optimal number of neurons in hidden layers calculated by optimizers

Optimizer	**AOA**			**BBO**		
Hidden layer No.	1	2	3	1	2	3
Optimal neuron No.	30	30	30	18	16	8
	-	30	14	-	8	24
	-	-	30	-	-	15

As shown in Table 3, the BBO optimizer needs a low number of hidden layer neurons. Except for the second layer in the three layers modeling, all hidden layers in BBO can manage the computation process with a low number of neurons.

4. Conclusions

The main goal of the research has been to discover the feasiability of application to use an integrated inteligent neural network for predicting the pile settlement (PS) in the project of Klang Valley Mass Rapid Transit (KVMRT) transportation network, used in country of KualaLumpur, in the city of Malaysia. The diverse hidden layer number (from 1 - 3) got investigated that would have a vast, correct, and authentic outcomes, in which Arithmetic Optimization Algorithm (AOA) and Biogeography-Based Optimization (BBO) were operated to justify the optimum number of neurons fro the layers of hidden type. For this research, variants, as the pile length beneath the surface-soil to length under the rock, whole pillar length to the crosssection diameter, standard penetration test, the parameter ofstrength of uniaxial compressive, the variable of ultimate capacity of bearing as entering variables, and PS for the outcome. The objective outcomes have been brought in following:

- The outcomes of developed integrated frameworks (MLP-BBO and MLP-AOA) in estimating the PS justify significant capacity over the phase of train and validation stage to whole integrated framework of MLP. By considering the comparison of actual PS with the estimated movements by the framework MLP-BBO and the MLP-AOA algorithms has been performed that the developed models have the best R^2 at 0.9549 for training data and 0.9667 for the testing phase. Regarding the MLP-BBO model in the training phase, the MLP model with one hidden layer has the highest R^2 at 0.9447, while the lowest value was MLP (0.9229). For the MLP-AOA model, opposite the BBO model, a model with one hidden layer has the best R^2, but the MLP-BBO resulted in the low correlation value.
- The MLP-BBO model has the highest R2 computed on 0.9667 (best value between all models with different hidden layers) and the lowest R2 value of 0.9447 for the testing phase. For the calibration step, suitable values for *RMSE* belonged to AOA with the *RMSE* equals 0.7788, including one hidden layer, while BBO has the large value of *RMSE* with 1.0063. However, in the testing phase, the BBO model with three hidden layers has the best values for all indices, making it the proposed MLP model with three hidden layers in the MLP-BBO framework.
- In the front side, despite the MLP models optimized with the AOA have authentic efficiency, while the MLP-AOA framework led to lower efficiency than BBO ones. With the all indicators, the MLP-BBO could outperform other ones.
- As it is clear from the graphs in Fig. 8, for whole advanced integrated MLP framework, evaluated PS values depict outstanding agreement with measured rates, demonstrating checked integrated algorithms capability to estimate the pile movement accurately.
- The given error distribution figures represent that error distribution curves are like the Gaussian bell; but, the error ranges around the zero line for MLP-BBO in three hidden layers is higher than other models, which is considered the most suitable model. Therefore, the BBO optimization algorithm is recognized as more capable than AOA in computing the optimal neuron number for hidden layers.

REFERENCES

[1] M. F. Randolph and C. P. Wroth, “Analysis of Deformation of Vertically Loaded Piles,” *Journal of the Geotechnical Engineering Division*, vol. 104, no. 12, pp. 1465–1488, Dec. 1978, doi: 10.1061/AJGEB6.0000729.

[2] C. W. W. Ng, T. L. Y. Yau, J. H. M. Li, and W. H. Tang, “Side Resistance of Large Diameter Bored Piles Socketed into Decomposed Rocks,” *Journal of Geotechnical and Geoenvironmental Engineering*, vol. 127, no. 8, pp. 642–657, Aug. 2001, doi: 10.1061/(ASCE)1090-0241(2001)127:8(642).

[3] M. Esmaeili-Falak, H. Katebi, M. Vadiati, and J. Adamowski, “Predicting triaxial compressive strength and Young’s modulus of frozen sand using artificial intelligence methods,” *Journal of Cold Regions Engineering*, vol. 33, no. 3, p. 4019007, 2019.

[4] H. M. Coyle and L. C. Reese, “Load Transfer for Axially Loaded Piles in Clay,” *Journal of the Soil Mechanics and Foundations Division*, vol. 92, no. 2, pp. 1–26, Mar. 1966, doi: 10.1061/JSFEAQ.0000850.

[5] Q. Zhang and Z. Zhang, "A simplified nonlinear approach for single pile settlement analysis," *Canadian Geotechnical Journal*, vol. 49, no. 11, pp. 1256–1266, Nov. 2012, doi: 10.1139/t11-110.
[6] M. Xu, P. Ni, G. Mei, and Y. Zhao, "Load-settlement behaviour of bored piles with loose sediments at the pile tip: Experimental, numerical and analytical study," *Comput Geotech*, vol. 102, pp. 92–101, Oct. 2018, doi: 10.1016/j.compgeo.2018.06.010.
[7] P. Ni, L. Song, G. Mei, and Y. Zhao, "Generalized nonlinear softening load-transfer model for axially loaded piles," *International Journal of Geomechanics*, vol. 17, no. 8, p. 4017019, 2017.
[8] W. D. Guo and M. F. Randolph, "Rationality of load transfer approach for pile analysis," *Comput Geotech*, vol. 23, no. 1–2, pp. 85–112, Jul. 1998, doi: 10.1016/S0266-352X (98)00010-X.
[9] H. G. Poulos and E. H. Davis, *Pile foundation analysis and design*, no. Monograph. 1980.
[10] M. A. Shahin, "Load–settlement modeling of axially loaded steel driven piles using CPT-based recurrent neural networks," *Soils and Foundations*, vol. 54, no. 3, pp. 515–522, Jun. 2014, doi: 10.1016/j.sandf.2014.04.015.
[11] K. Y. Lo and A. G. Stermac, "Induced pore pressures during pile-driving operations," 1965.
[12] O. Orrje and B. B. Broms, "Effects of Pile Driving on Soil Properties," *Journal of the Soil Mechanics and Foundations Division*, vol. 93, no. 5, pp. 59–73, Sep. 1967, doi: 10.1061/JSFEAQ.0001044.
[13] T. H. Hanna, "The Measurement of Pore Water Pressures Adjacent to a Driven Pile," *Canadian Geotechnical Journal*, vol. 4, no. 3, pp. 313–325, Aug. 1967, doi: 10.1139/t67-053.
[14] B. H. Fellenius and B. B. Broms, "Negative skin friction for long piles driven in clay. 7th Intern," 1969.
[15] B. H. Fellenius, "Results from long-term measurement in piles of drag load and downdrag," *Canadian Geotechnical Journal*, vol. 43, no. 4, pp. 409–430, Apr. 2006, doi: 10.1139/t06-009.
[16] M. Pal and S. Deswal, "Modelling pile capacity using Gaussian process regression," *Comput Geotech*, vol. 37, no. 7–8, pp. 942–947, 2010.
[17] P. Samui, "Determination of friction capacity of driven pile in clay using Gaussian process regression (GPR), and minimax probability machine regression (MPMR)," *Geotechnical and Geological Engineering*, vol. 37, no. 5, pp. 4643–4647, 2019.
[18] E. Momeni, M. B. Dowlatshahi, F. Omidinasab, H. Maizir, and D. J. Armaghani, "Gaussian process regression technique to estimate the pile bearing capacity," *Arab J Sci Eng*, vol. 45, no. 10, pp. 8255–8267, 2020.
[19] W. G. Zhang and A. T. C. Goh, "Multivariate adaptive regression splines for analysis of geotechnical engineering systems," *Comput Geotech*, vol. 48, pp. 82–95, 2013.
[20] R. S. Benemaran and M. Esmaeili-Falak, "Optimization of cost and mechanical properties of concrete with admixtures using MARS and PSO," *Computers and Concrete*, vol. 26, no. 4, pp. 309–316, 2020.
[21] L. Teodorescu and D. Sherwood, "High energy physics event selection with gene expression programming," *Comput Phys Commun*, vol. 178, no. 6, pp. 409–419, 2008.
[22] T.-T. Le and M. V. Le, "Development of user-friendly kernel-based Gaussian process regression model for prediction of load-bearing capacity of square concrete-filled steel tubular members," *Mater Struct*, vol. 54, no. 2, pp. 1–24, 2021.
[23] I. Alkroosh and H. Nikraz, "Correlation of pile axial capacity and CPT data using gene expression programming," *Geotechnical and Geological Engineering*, vol. 29, no. 5, pp. 725–748, 2011.
[24] S. R. Dindarloo, "Prediction of blast-induced ground vibrations via genetic programming," *Int J Min Sci Technol*, vol. 25, no. 6, pp. 1011–1015, 2015.
[25] A. T. C. Goh, "Pile Driving Records Reanalyzed Using Neural Networks," *Journal of Geotechnical Engineering*, vol. 122, no. 6, pp. 492–495, Jun. 1996, doi: 10.1061/(ASCE)0733-9410(1996)122:6(492).
[26] C. I. Teh, K. S. Wong, A. T. C. Goh, and S. Jaritngam, "Prediction of pile capacity using neural networks," *Journal of computing in civil engineering*, vol. 11, no. 2, pp. 129–138, 1997.
[27] F. Pooya Nejad, M. B. Jaksa, M. Kakhi, and B. A. McCabe, "Prediction of pile settlement using artificial neural networks based on standard penetration test data," *Comput Geotech*, vol. 36, no. 7, pp. 1125–1133, Sep. 2009, doi: 10.1016/j.compgeo.2009.04.003.
[28] A. Soleimanbeigi and N. Hataf, "Prediction of settlement of shallow foundations on reinforced soils using neural networks," *Geosynth Int*, vol. 13, no. 4, pp. 161–170, 2006.
[29] M. A. Shahin, H. R. Maier, and M. B. Jaksa, "Predicting settlement of shallow foundations using neural networks," *Journal of Geotechnical and Geoenvironmental Engineering*, vol. 128, no. 9, pp. 785–793, 2002.
[30] A. Nassr, M. Esmaeili-Falak, H. Katebi, and A. Javadi, "A new approach to modeling the behavior of frozen soils," *Eng Geol*, vol. 246, pp. 82–90, 2018.
[31] H. Rezaei, R. Nazir, and E. Momeni, "Bearing capacity of thin-walled shallow foundations: an experimental and artificial intelligence-based study," *Journal of Zhejiang University-SCIENCE A*, vol. 17, no. 4, pp. 273–285, 2016.
[32] S. Yagiz, E. A. Sezer, and C. Gokceoglu, "Artificial neural networks and nonlinear regression techniques to assess the influence of slake durability cycles on the prediction of uniaxial compressive strength and modulus of elasticity for carbonate rocks," *Int J Numer Anal Methods Geomech*, vol. 36, no. 14, pp. 1636–1650, 2012.
[33] E. Momeni, R. Nazir, D. J. Armaghani, and H. Maizir, "Application of artificial neural network for predicting shaft and tip resistances of concrete piles," *Earth Sciences Research Journal*, vol. 19, no. 1, pp. 85–93, 2015.
[34] M. Khandelwal and T. N. Singh, "Evaluation of blast-induced ground vibration predictors," *Soil Dynamics and Earthquake Engineering*, vol. 27, no. 2, pp. 116–125, 2007.
[35] D. J. Armaghani, M. F. M. Amin, S. Yagiz, R. S. Faradonbeh, and R. A. Abdullah, "Prediction of the uniaxial compressive strength of sandstone using various modeling

techniques," *International Journal of Rock Mechanics and Mining Sciences*, vol. 85, pp. 174–186, 2016.
[36] W. Gao, J. L. G. Guirao, M. Abdel-Aty, and W. Xi, "An independent set degree condition for fractional critical deleted graphs," *Discrete & continuous dynamical systems-S*, vol. 12, no. 4 & 5, p. 877, 2019.
[37] J. O. Agushaka and A. E. Ezugwu, "Advanced arithmetic optimization algorithm for solving mechanical engineering design problems," *PLoS One*, vol. 16, no. 8, p. e0255703, Aug. 2021, doi: 10.1371/journal.pone.0255703.
[38] S. Khatir, S. Tiachacht, C. Le Thanh, E. Ghandourah, S. Mirjalili, and M. Abdel Wahab, "An improved Artificial Neural Network using Arithmetic Optimization Algorithm for damage assessment in FGM composite plates," *Compos Struct*, vol. 273, p. 114287, Oct. 2021, doi: 10.1016/j.compstruct.2021.114287.
[39] A. Kaveh and K. B. Hamedani, "Improved arithmetic optimization algorithm and its application to discrete structural optimization," in *Structures*, 2022, vol. 35, pp. 748–764.
[40] H. Moayedi, A. Osouli, D. T. Bui, L. Kok Foong, H. Nguyen, and B. Kalantar, "Two novel neural-evolutionary predictive techniques of dragonfly algorithm (DA) and biogeography-based optimization (BBO) for landslide susceptibility analysis," *Geomatics, Natural Hazards and Risk*, vol. 10, no. 1, pp. 2429–2453, Jan. 2019, doi: 10.1080/19475705.2019.1699608.
[41] A. W. Hatheway, "The complete ISRM suggested methods for rock characterization, testing and monitoring; 1974–2006." Association of Environmental & Engineering Geologists, 2009.
[42] L. Abualigah, A. Diabat, S. Mirjalili, M. Abd Elaziz, and A. H. Gandomi, "The Arithmetic Optimization Algorithm," *Comput Methods Appl Mech Eng*, vol. 376, p. 113609, Apr. 2021, doi: 10.1016/j.cma.2020.113609.
[43] D. Simon, "Biogeography-based optimization," *IEEE transactions on evolutionary computation*, vol. 12, no. 6, pp. 702–713, 2008.
[44] W. Sun, D. Liu, J. Wen, and Z. Wu, "Modeling of MEMS gyroscope random errors based on grey model and RBF neural network," *J. Navig. Position*, vol. 5, pp. 9–13, 2017.
[45] S. Seshagiri and H. K. Khalil, "Output feedback control of nonlinear systems using RBF neural networks," *IEEE Trans Neural Netw*, vol. 11, no. 1, pp. 69–79, 2000.
[46] I. A. Basheer and M. Hajmeer, "Artificial neural networks: fundamentals, computing, design, and application," *J Microbiol Methods*, vol. 43, no. 1, pp. 3–31, 2000.
[47] B. Gordan, M. Koopialipoor, A. Clementking, H. Tootoonchi, and E. T. Mohamad, "Estimating and optimizing safety factors of retaining wall through neural network and bee colony techniques," *Eng Comput*, vol. 35, no. 3, pp. 945–954, 2019.